

Article

Tsunami Boulders on the Rocky Coasts of Ibiza and Formentera (Balearic Islands)

Francesc Xavier Roig-Munar ¹, Antonio Rodríguez-Perea ², José Angel Martín-Prieto ^{1,2}, Bernadi Gelabert ^{3,*} and Joan Manuel Vilaplana ⁴

¹ QU4TRE Consultoria Ambiental, C/Carritxaret 18-apt. 6, es Migjorn Gran, 07749 Menorca, Spain; xiscoroig@gmail.com (F.X.R.-M.); josean33@gmail.com (J.A.M.-P.)

² Departamento de Geografía, Universitat de les Illes Balears, Palma de Mallorca, Carretera de Valldemossa km 7,5, 07122 Palma de Mallorca, Spain; arperea2@gmail.com

³ Departamento de Biología, Universitat de les Illes Balears, Palma de Mallorca, Carretera de Valldemossa, km 7,5, 07122 Palma de Mallorca, Spain

⁴ Dpto. de Dinàmica de la Terra i de l'Oceà, Grupo RISKINAT, Geomodels, Universitat de Barcelona, Martí i Franquès, s/n. 08028 Barcelona, Spain; nue.vilaplana@ub.edu

* Correspondence: bernadi.gelabert@uib.es; Tel.: +34-97117237

Received: 5 June 2019; Accepted: 6 September 2019; Published: 20 September 2019



Abstract: Large boulders have been found in marine cliffs from 7 study sites on Ibiza and Formentera Islands (Balearic Islands, Western Mediterranean). These large boulders of up to 43 t are located on platforms that form the rocky coastline of Ibiza and Formentera, several tens of meters from the edge of the cliff, up to 11 m above sea level and several kilometers away from any inland escarpment. Despite that storm wave height and energy are higher from the northern direction, the largest boulders are located in the southern part of the islands. The boulders are located in the places where numerical models of tsunami simulation from submarine earthquakes on the North African coast predict tsunami impact on these two islands. According to radiocarbon data and rate of growth of dissolution pans, the ages of the boulders range between 1750 AD and 1870 AD. Documentary sources also confirm a huge tsunami affecting the SE coast of Majorca (the largest Balearic Island) in 1756. The distribution of the boulders sites along the islands, the direction of imbrication and the run-up necessary for their placement suggest that they were transported from northern African tsunami waves that hit the coastline of Ibiza and Formentera Islands.

Keywords: tsunami boulders; coastal cliff; Ibiza; Formentera

1. Introduction

There is evidence that rocky coasts are sensitive to high-energy events such as storms [1], hurricanes, typhoons, or cyclones [2] and tsunamis [3]. One of the main effects of the tsunamis on rocky shores is represented by the presence of mega boulders displaced inland [4]. The identification of these boulders transported by tsunamis or storms is essential for the recognition of the occurrence of events produced in the past [5], as well as to estimate the hydraulic properties that have given rise to these [6]. The distinction of boulders associated with tsunamis is based on a set of sedimentological, morphological, chronological, stratigraphic, and organizational criteria that can be analyzed in detail. Being the deposits of boulders imbricated and aligned along the coast, they show clear transport indicators associated with tsunamis [7]. In the last decade, the debate regarding on the transport of boulders to discern their origin between tsunamis and large storms has forced to researchers to further consider in more detail the role of storms on the rocky coasts [8]. Some equations have been developed to estimate the over-elevation by lift or run-up necessary on a block, under three assumptions: submerged boulders, subaerial boulders, and boulders delimited by joints or fractures [9,10].

In the Western Mediterranean, documented examples of boulders displaced on rocky shores by historical tsunamis are numerous and have been compiled by [11,12], and expanded by [13,14]. These are boulders of metric order, plucked from the edge of the cliff and transported inland, presenting geomorphological, orientation and imbrication characteristics that allow them to be differentiated from those related to other sedimentary environments. The presence of boulders on the rocky coasts of Majorca (the largest of the Balearic Islands) was studied by [11,15,16]. Reference [17,18] analyzed boulders on the coasts of Minorca and Majorca (see Supplementary Materials), applying different equations to distinguish between the boulders associated with storms and boulders associated with tsunamis, and outlining its relation with the trajectories of tsunamis from the N of Africa [19]. In this paper we document, for the first time, the presence of large boulders on the coasts of Ibiza Island (located at the S of the Balearic Islands). The main goal of this article is to demonstrate that some of these boulders, located close to the coastal cliffs of Ibiza and Formentera Islands, were transported and deposited by tsunamis that occurred in the recent past and mostly originated from submarine earthquakes at the Algerian coast.

1.1. Geological Framework

The island of Ibiza is located in the south-western Mediterranean Sea and is the third-largest (571 km²) and most Westerly Island of the Balearic Islands (Figure 1). Geological structure of the island is composed of a series of thrust sheets (mainly of Middle Triassic to Middle Miocene carbonate deposits) formed during the Alpine compression (Upper Oligocene to Middle Miocene) and trending NE-SW [20]. These thrust sheets correspond to the northeasterly continuation of the Subbetic Ranges in the southern Iberian Peninsula. Bedrock lithology of Ibiza is composed mainly of Miocene and Mesozoic carbonate rocks [21]. Muschelkalk limestone and dolomite, as well as Keuper marls and clays, constitute the Triassic materials of the island, whereas Jurassic limestone and dolomites and Cretaceous to Middle Miocene limestone overlie the Triassic materials and constitute the significant reliefs of the island. Quaternary fluvial, alluvial and colluvial sediments fill the central basins, whereas Pleistocene coastal successions characterized by shallow-marine to coastal aeolian and colluvial deposits crop out patchily along the cliffed coasts [22].

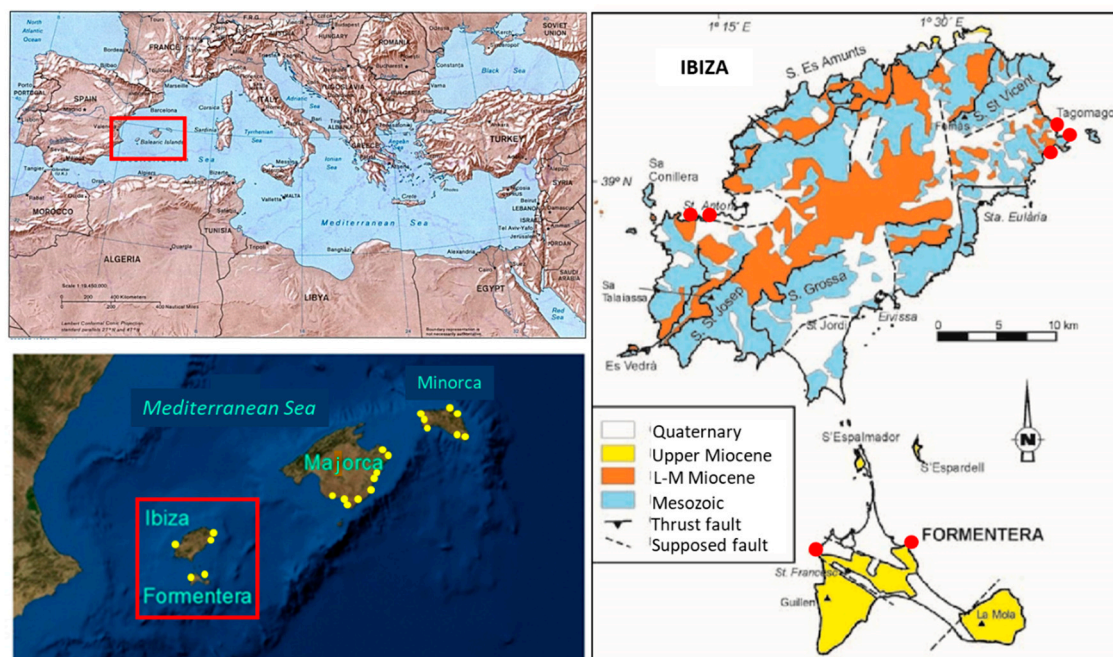


Figure 1. Setting and geological framework of Ibiza and Formentera Islands. Red and yellow dots correspond to the boulder outcrops analyzed.

In Ibiza, the main outcrops are found on the west coast, west of Sant Antoni, and on the northeast coast, close to Santa Eularia (Figures 1 and 2). West of Sant Antoni, analyzed boulders are set in two different locations: first, above Punta Pedrera, a small peninsula 16.5 m a.s.l (above sea level) formed by Pleistocene colluvial and alluvial sediments, and secondly, in a coastal ditch two meters a.s.l. (Sant Antoni) formed by Pleistocene aeolianites. Northeast of Santa Eularia, analyzed boulders are also located in three settings: Ses Eres Roges shows boulders on Pleistocene aeolianites, in Pou des Lleó the materials are Middle Triassic limestones and in Punta Arabí boulders are formed by Cretaceous limestones.

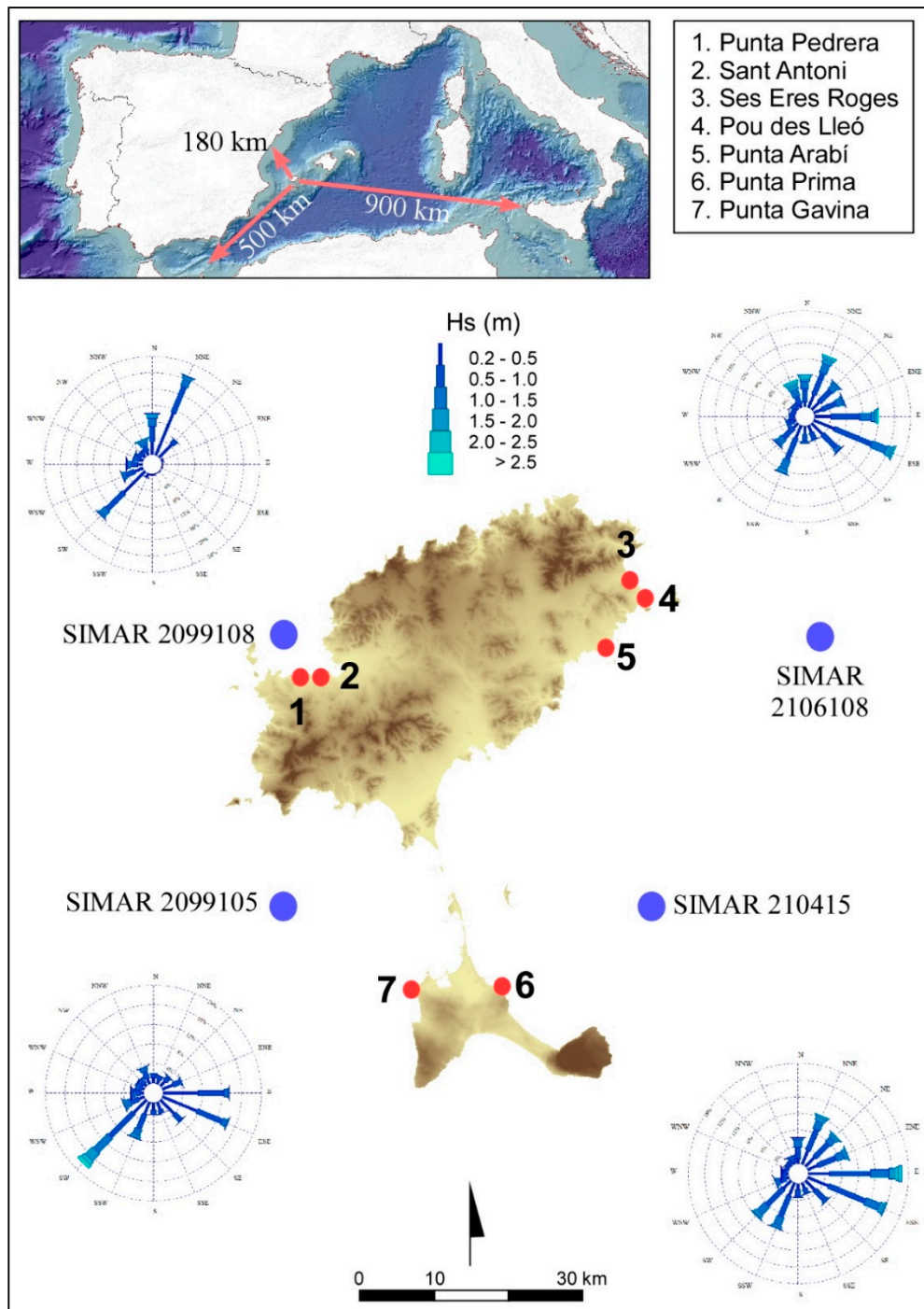


Figure 2. Wave fetch affecting Ibiza and Formentera Islands. Roses of wave directions and wave height frequencies for each SIMAR points. Red points correspond to boulder outcrops analyzed.

Physiographically, the island of Formentera is very different from Ibiza: Formentera constitutes a graben, whereas Ibiza is the corresponding horst. Formentera is constituted of four domains (Figure 1). At its eastern and western ends rise two promontories, meanwhile, between them, there is a dune ridge NW-SE, which is less than 2 km wide. The eastern promontory, La Mola, reaches an altitude of 197 m on a gently undulating tabular platform, with cliffs that surpass 100 m. The western promontory, of Barbaria, tilted towards the NNE, reaches 108 m of altitude at its extreme SSW. Geologically, the island is constituted by a carbonate set of reef origin deposited during the Tortonian, on which alluvial deposits, soils and wind accumulations are superimposed. A fracture under an extensive regime gave rise to a network of normal faults, the result of which was the individualization of the promontories of La Mola and Barbaria [23]. The Miocene materials of the Tortonian are found in a part of the coast, little deformed, where the clays, sands, breccias, and limestones constitute a heterogeneous group. Several islands and islets insinuate the connection between the northern dune ridge and Ibiza, constituting the intermediate archipelago between both islands, which is composed of the remains emerged from a partially submerged threshold and whose depth does not reach 10 m.

In Formentera island, boulders remain in the areas of Punta Prima, in the E of the island, and Punta de sa Gavina, in the W (Figure 2) [24,25]. These two areas, formed by Miocene calcareous materials, stand out for presenting metric size boulders at distances tens of meters away from the cliff edge and with heights higher than 11 m a.s.l. The sites are associated with several littoral terraces with heights between 5 and 15 m a.s.l.

1.2. Wave Climate

The Mediterranean basin is characterized by a highly indented coastline that creates some small and well-defined sub-basins, where wave energy is conditioned by wind speed and limited fetches [26]. In the western Mediterranean, the most intense waves come from the NE [27], although the NW also generates strong waves between the Balearics, Corsica, and Sardinia as well [28].

Tidal regime observed at Harbors of Formentera and Ibiza is about 0.41 m [29]; hence, the coastal area subjected to this study can be considered micro-tidal and low and high pressures can be considered responsible of some more significant oscillations.

The wave data correspond, on the one hand, to the Puertos del Estado digital buoy system; it is formed by time series of wind and wave parameters, at some points, from numerical modelling (called SIMAR points) and, on the other, to the analysis of wave data carried out by [30]. In the first case, these figures are average values for the four SIMAR points used. According to the analysis of Puertos del Estado, the distribution chosen to describe the average wave series regime is that of Weibull, Hs is the average height of the highest third of waves, while Tp is the period of the group of waves with more energy.

Data from SIMAR points 2099108 and 2106108 (placed in the W and E, respectively) for the period 1958–2018 with the reliability of 99.68% [29] were analyzed (Figure 2, Table 1). The SIMAR data set consists of a time series of wind and wave parameters obtained from numerical modeling [29].

Table 1. Wave data from SIMAR points (Figure 2). Fetch in kilometers; Hs, significant wave height in meters; Tp, wave period in seconds (www.puertos.es); Hs50, significant wave height for 50 years’ return period according to [30] (for location see Figure 2).

SIMAR	Location	Water Depth	Fetch	Fetch Direction	Tp	Hs	Hs50
2099108	1.25 E–39.00 N	95 m	180	NW	10.99	5.17	11
2106108	1.83 E–39.00 N	150 m	920	E	10.46	5.83	11
2099105	1.25 E–37.75 N	108 m	500	SW	11.33	6.04	7
2104105	1.67 E–38.75 N	325 m	900	E	10.71	5.83	11

The wave climate of Ibiza differs from one coast to the other, mainly in the length of the fetch. The shorter corresponds to the W with a maximum of 180 km to the NNW, and the swell is characterized by a significant wave (Hs) where 86.02% is lower than 1 m, and only 0.006% is higher than 6 m, the

87.26% of the peak period (T_p) is inferior to 7 s. The main component direction is from NNW, with a frequency of 24%. The East sector of Ibiza has the biggest fetch to the E with 920 km. It is characterized by an H_s , where 72.56% is lower than 1 m. Concerning the peak period, 87.2% is lower than 7 s, and only 0.55% of the record exceeds 10 s. The main component direction is from the ESE and E, with a frequency of 18% and 16%, respectively.

In Formentera, the maritime climate has similar characteristics to the neighbor Ibiza. On the western coast, the maximum fetch is 500 km towards the SW, and the swell is characterized by a significant wave height (H_s) with a frequency of 83.8% less than 1 m, and a peak period of 73.7% less than 6 s, where only the H_s exceeds 6 m by 0.20%. The main component of its address is SW, with a frequency that reaches 25%. Its eastern coast has a maximum fetch of 900 km towards the E, with an H_s less than 1 m in 75.2% of cases, where only 0.11% of the time exceeds 6 m. The peak period is characterized by 63.4% less than 6 s, and the main component of its direction is from E, with a frequency of 28%.

Reference [30] made an estimate of the spatial variability of the recurrence of 50 years for the significant wave height of the Balearic Sea, obtaining estimates around 11 m in the eastern sector (for both islands) and 7 m in the western of Formentera and 11 in western Ibiza (Table 1).

1.3. Tsunamis in Ibiza and Formentera

According to [31], the primary tsunamigenic source in the Western Mediterranean is located offshore at the north of Algeria (Figure 3), which is characterized by compressive tectonics (the North Algerian fold and thrust belt). Another minor tsunamigenic area is the Alboran Basin, characterized by transcurrent and transpressive tectonics.

The last tsunami registered affecting the Balearic Islands was in 2003 (May 21). This tsunami was due to an earthquake, generated by a reverse fault, with a magnitude of 6.9 in Zemmouri (Algeria). Despite being a moderate magnitude earthquake, it generated a tsunami observed on the coasts of Algeria, Spain, France, and Italy. The maximum lift by run-up measured in the Balearic Islands was 3 m in Sant Antoni (Ibiza), and material damage occurred in the ports of Majorca, Minorca, and Ibiza. The propagation of this 2003 tsunami was modeled by [19,32–34], including in these study data of wave trajectories, location of tsunami impact areas, wave travel times and wave elevation (Figure 3).

Thus, there is currently seismic activity at the bottom of the Algerian Basin that gives rise to tsunamis affecting the coast of the Balearic Islands. In the recent past, in the last 500 years, there have been tsunamis affecting the Balearic Islands (Table 2). Among the historical records of massive wave phenomena that have affected the Balearic Islands, some episodes can be attributed to tsunamis. In 1856, the chronicles were written by [35] record an extraordinary sea rise in the Port of Maó (Minorca Island, Figure 1) that destroys several moorings. In 1918, a new 'seismic wave' floods the Port of Maó, following an earthquake offshore the Algerian coast [35]. There are also historical records reporting a flooding event with a run-in up to 2 km inland and a run-up up to 45 m at the east coast of Majorca (the largest of the Balearic Islands) in 1756 [35].

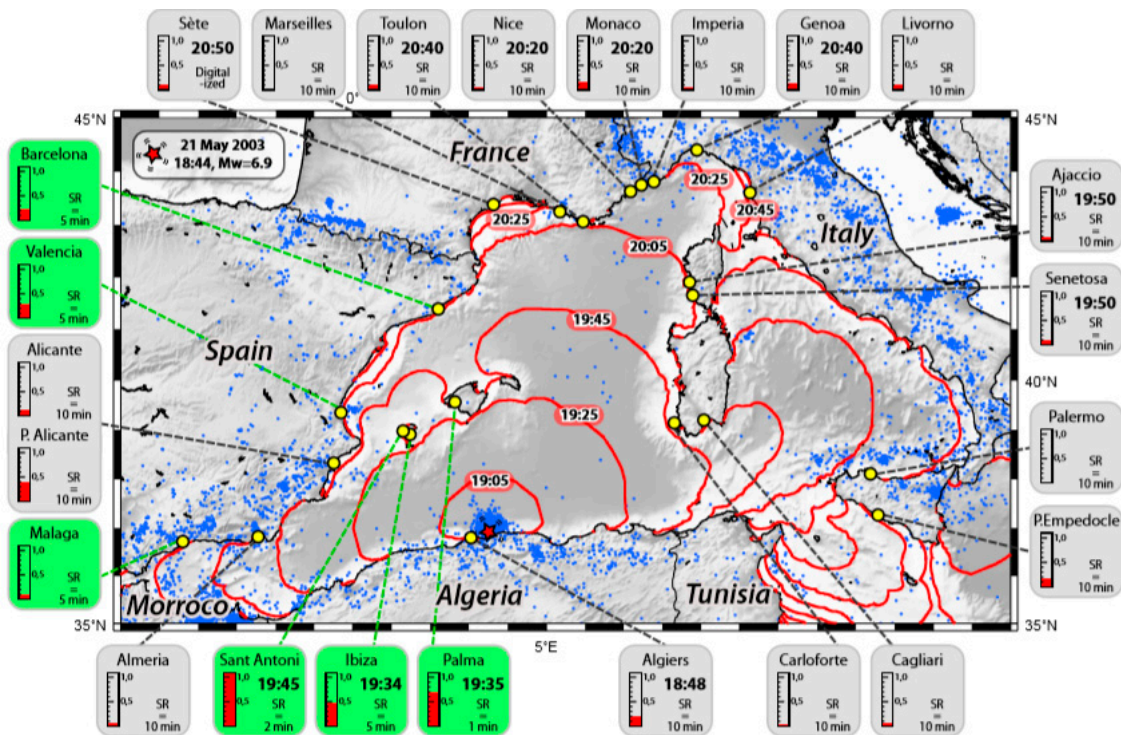


Figure 3. Modeling estimated travel time and impact areas based on the tsunami records of 21 May, 2003 [34]. Blue dots record background seismicity from 1998–2005 (CSEM-EMSC). Green rectangles record tide gauges with precise sampling rates.

Table 2. Historical tsunamis phenomena were impacting in the Balearic Islands, modified from [36]. Information sources (IS): (1) [35] and (2) [37,38].

Data	Affected Area	Phenomenon	IS
1660	Majorca, Palma, Campos	Earthquake and tsunami	1
1721	Balearic Islands	Earthquake and seawater withdrawal	1
1756	Majorca, Santanyi	Tsunami and big waves	1
1756	Balearic Islands	Tsunami and flooded coasts	2
1790	Alboran Sea	Tsunami	2
1804	Alboran Sea	Tsunami	2
1856	Minorca, Maó	Tsunami and seismic wave	1
1856	Algeria	Tsunami	2
1885	Algeria	Sea level changes	2
1891	Algeria	Tsunami	2
1918	Minorca, Maó	Seismic wave	1
2003	Algeria	Earthquake (7.0) and tsunami	2

Reference [33] modeled the tsunami-related with the 1856 offshore Djijelli (Algeria) earthquake, with particular attention towards its impact on the Balearic Islands. The study concludes that the wave arrivals in the Balearic Islands concerning the 2003 tsunami are reported in the same areas than for the modeled 1856 results, highlighting the highest exposure of the southeastern coasts of the Balearic Islands to tsunamis coming from central and eastern Algeria.

Reference [19] used 22 tsunamigenic seismic sources to estimate the tsunami threat over the Spanish Mediterranean coast of the Iberian Peninsula and the Balearic Islands. They modeled tsunamis generated from seismic sources of N Africa, from the Alboran Sea to N of Algeria. According to [19], the sources of the N of Algeria S-1 and S-2 (Figure 4) are those that most affect the coasts of Ibiza and Formentera and have maximum wave height values of more than 2 m in the S of both islands, especially S of Formentera, where values higher than 4 m reach the Cap de Barbara. In addition to

these two principal sources, sources S-3, S-4, and S-6 can also generate wave elevations close to 2 m. The seismic sources S-0 to S-9 are located N of Algeria (S-0 to the west and, progressively, S-9 to the east, Figure 4). The model considers a 7.3 earthquake magnitude and the seismic sources S-0 to S-9 consists of low-angle reverse faults, 55 km in length, verging towards the N and NW.

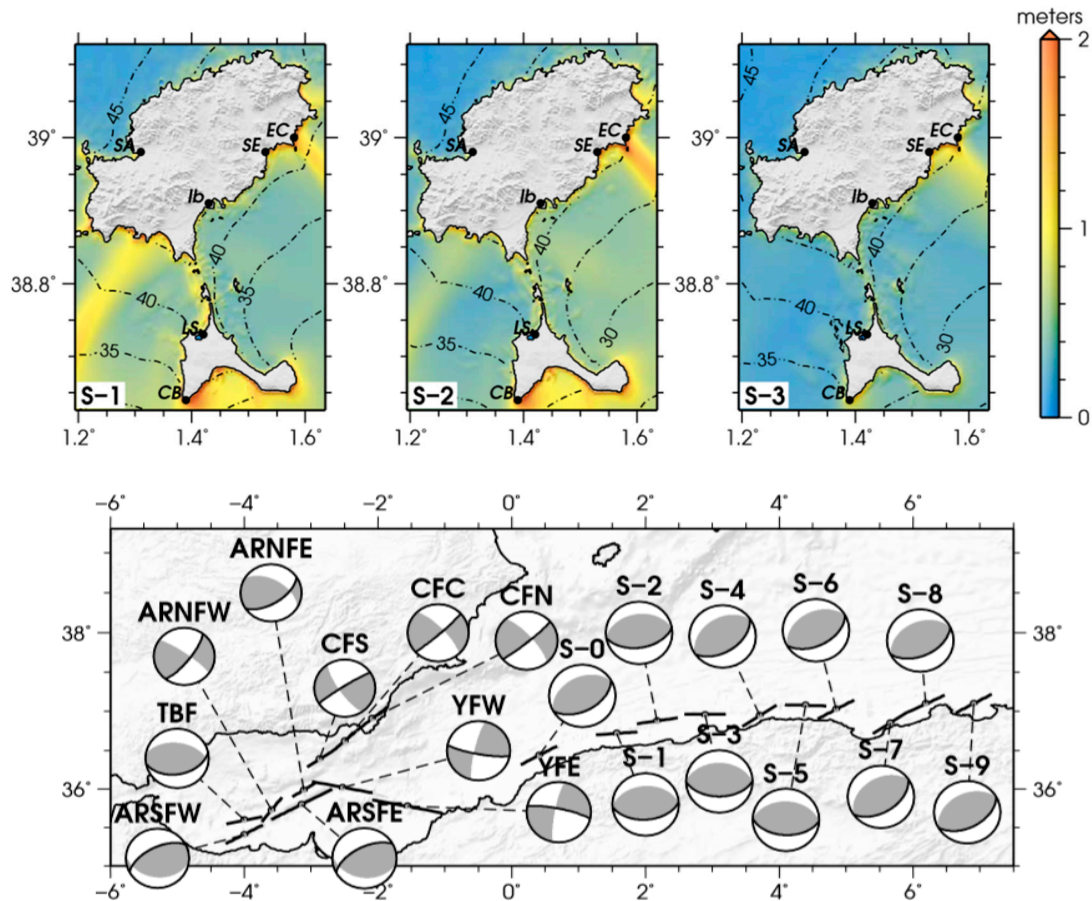


Figure 4. Maps of maximum wave elevation and estimated travel times of the tsunami in the islands of Ibiza and Formentera, according to the three of the tsunami sources defined by [19]. Below, seismic sources modelled as probable tsunamigenic worst cases for the westernmost Mediterranean coast (taken from [13]). The thick lines are the surface trace of the faults and the focal mechanisms represent the rupture characteristics. The black line of each double couple is the fault plane.

2. Methods

For each area the following tasks have been carried out:

1. Geomorphological map of the coastal areas at a 1:1000 scale.
2. Topographic and bathymetric profiles perpendicular to the coast were made for each area. Profiles were prepared from the -30 m isobaths to the start of the terrestrial vegetation cover. Topographic data from [39] and the bathymetric data from [40] were used.
3. The dimensions of the boulders were measured (a, b, c axis on behalf of the long, intermediate, and short axis, respectively). According to [10], the volume of a boulder that is based on a multiplication of the central axis (V_{abc}) overestimates the actual volume and produces an overestimation of the wave energy and wave heights needed for their transport. Those authors, through a complex process of digital photography, [10] estimate the real volume as 49% of the V_{abc} . To estimate that percentage for our measured volumes, we did a test on several boulders through decomposing the volume of the block in measurable parallelepipeds that by addition

represent more accurately the real volume of the block. On average, the volume by triangulation was 68% of the V_{abc} . This percentage has been applied to all of the analyzed blocks.

4. The height above mean sea level of the boulders, and their distance from the edge of the cliff were also measured as well. Their orientation and imbrication were considered, and the geomorphological context in which they were found. Isolated boulders, an imbricated group of boulders or ridges of imbricate boulders, were also registered.

Other qualitative observations were taken into account:

- (a) The relation of the boulders with its source area (based on bed thickness, facies, and lithology), and the presence of fractures that can promote detachment of the boulders,
- (b) The presence of encrusted marine fauna indicating the origin of the boulder before its displacement,
- (c) The presence of pre-detachment and post-detachment solution pans which have been used as age indicators for boulder emplacement,
- (d) The degree of rounding of the boulders, presence or absence of another type of sediment as well as the presence of abrasion surfaces due to boulder quarrying and transport,
- (e) The presence of flow-outs, areas with denudated beds forming channels over the cliff, favoring the entry and acceleration of the water flows and leaving a boulder ridge at its front.

To have an approximate hydrodynamic value of storm or tsunami for quarrying, transport, and deposition of the boulders, equations of [5,10] were applied under three different pre-settings: submerged, subaerial and joint-bounded boulders. The Transport Figure values of [11] were calculated (Table 3). Because most of the observed boulders were detached from the edge of the cliff joint-bounded and subaerial scenarios must be considered. Two boulders showed features (incrusted marine fauna or notch fragments) indicating that they were submerged in their origin.

Table 3. Equations used in the analysis of Ibiza and Formentera boulders. $\rho_s = 1.9 \text{ g/cm}^3$ for Quaternary boulders and 2.3 g/cm^3 for Jurassic boulders, $\rho_w = 1.027 \text{ g/mL}$, $C_d = 2$, $C_l = 0.178$, $C_m = 2$, $\ddot{u} = 1 \text{ m/s}^2$, $\mu = 1$, $q = 0.73$. Coefficient values according to [10].

		Ht		Hs		
Nott (2003) [9]	submerged	$Ht = [0,25(\rho_s - \rho_w/\rho_w) 2a]/[(C_d (ac/b^2)+ C_l)]$		$Hs = [(\rho_s - \rho_w/\rho_w) 2a]/[(C_d (ac/b^2)+ C_l)]$		
	subaerial	$Ht = [0,25 (\rho_s - \rho_w/\rho_w) [2a - C_m (a/b) (\ddot{u}/g)]/[C_d (ac/b^2)+ C_l]$		$Hs = [(\rho_s - \rho_w/\rho_w) [2a - 4C_m (a/b) (\ddot{u}/g)]/[C_d (ac/b^2)+ C_l]$		
	joint-bounded boulder	$Ht = [0,25 (\rho_s - \rho_w/\rho_w) a]/C_l$		$Hs = [(\rho_s - \rho_w/\rho_w) a]/C_l$		
Engel and May (2012) [10]	subaerial	$Ht = 0,5 \cdot \mu \cdot V \cdot \rho_b / C_D \cdot (a \cdot c \cdot q) \cdot \rho_w$		$Hs = 2 \cdot \mu \cdot V \cdot \rho_b / C_D \cdot (a \cdot c \cdot q) \cdot \rho_w$		
	joint-bounded boulder	$Ht = (\rho_b - \rho_w) \cdot V \cdot (\cos \theta + \mu \cdot \sin \theta) / 2 \cdot \rho_w \cdot C_L \cdot a \cdot b \cdot q$		$Hs = (\rho_b - \rho_w) \cdot V \cdot (\cos \theta + \mu \cdot \sin \theta) / 0.5 \cdot \rho_w \cdot C_L \cdot a \cdot b \cdot q$		
	Ht	tsunami height	a	the large axis of the boulder	C_d	coefficient of drag
	Hs	storm wave height	b	the medium axis of the boulder	C_l	coefficient of lift
	ρ_s	boulder density	c	the short axis of the boulder	C_m	coefficient of mass
	ρ_w	seawater density	g	force of gravity	\ddot{u}	the speed of water flow
	V	vol. abc of the boulder	q	boulder area coefficient	θ	cliff top steepness
	μ	boulder coefficient of friction				

Ref. [41] proposes a new equation to obtain the minimum tsunami height (HT) at the coastline which can move a joint-bounded boulder (JBB). This Nott-derived equation differs from the original concerning the relevance of the c-axis, which indicates the thickness of the boulder directly exposed to the wave impact. Ref. [42] also revised Nott’s equation, rearranging the lift area of the boulders in the subaerial and submerged scenarios and taking into account the effect of the slope at the pre-transport location for the joint-bounded scenario. The differences between the results obtained from Nott’s

equations and the revised equations of [42] were that the minimum flow velocity required to initiate the transport was reduced up to 56% for submerged boulders and up to 65% for joint-bounded blocks.

Reference [10] reconsider Nott's equations through a more accurate volume and density measurement and established equations to derive the minimum wave height of a tsunami (HT) or storm wave (HS) which is required to dislodge a particular subaerial or JBB boulder (Table 3).

Finally, we also used the Transport Figure (TF) equation of [11]. TF equation is the product of the height (H, in meters) of the boulder above sea level, its distance (D, in meters) from the edge of the cliff and its mass (M, in tons)

$$TF = M \cdot D \cdot H. \tag{1}$$

Transport figure is a simple, useful and essential formula because it is an indirect approach for establishing the energy required for the transport of the boulders: the heavier the boulders, the higher its elevation above sea level and the farther its distance to the cliff, the higher the energy required for its transport. Ref. [11] used the TF values in the southern and northern sector of Majorca for discerning the storm or tsunami origin of the boulders. According to these authors, $TF < 250$ corresponds to boulders transported by storms and $TF > 250$ matches to boulders transported by tsunamis. In this work, and in order to fall on the side of safety, it has been estimated that a $TF > 1000$ is indicative of tsunami. It is four times the considered value by previous authors, even when applying a significant reduction (32% of V_{abc}) in calculating the volume of the boulders.

We are aware than mathematical models are still in their initial stages and that the equations are under constant review and improvement. In selecting [5,10,11] formulas, we search to obtain an approximate value, even just an order of magnitude, for the height of the waves required for the boulder transport.

3. Results

3.1. Ibiza: Punta Pedrera

Boulders are located on a small peninsula formed by a Pleistocene tabular platform slightly tilted to the east (Figure 5). The cliff has a vertical profile that continues below the sea, followed by a gentle bathymetry. Boulders are distributed individually along with the tabular platform, although there are small groups of 3 to 4 imbricated boulders of small dimensions. Boulders do not show evidence of reworking. The average weight of the boulders is 8.4 t, and they are located at an average distance of 66 m from the cornice and at an average height of 10 m a.s.l. Maxim values of these figures are 43.2 t of weight, 11 m a.s.l., and 77 m from the cliff edge. Average orientation of the boulders is towards the NNW, while the dominant swell comes mainly from NE.

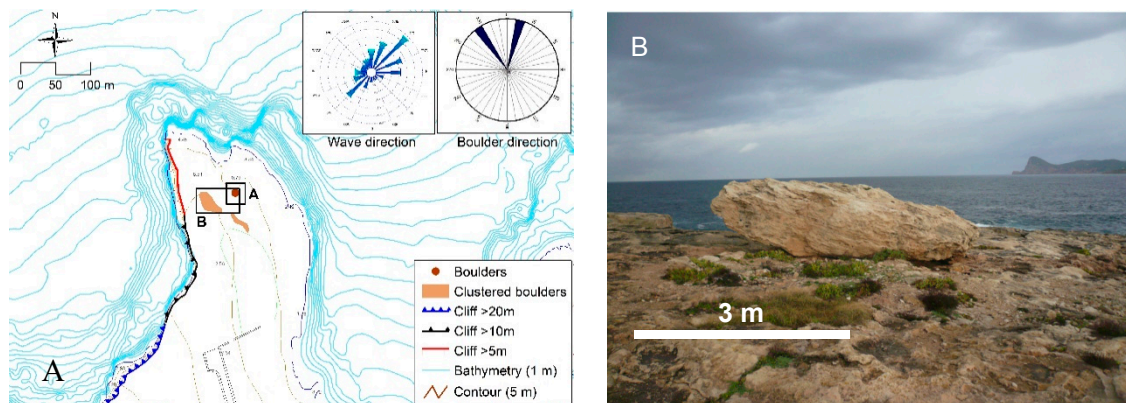


Figure 5. Cont.



Figure 5. (A) Geomorphological scheme of the Punta Pedrera area. Roses show the prevailing wave direction. (B) Large coastal boulder located 10 m a.s.l. (C) Boulder ridge at Punta Pedrera. Notice the person in the circle.

3.2. Ibiza: Sant Antoni

The boulders westward of Sant Antoni are located over a low-lying littoral terrace build on Pleistocene aeolianites (Figure 6). That terrace shows a gentle stratification towards the sea, which allows the progressive dismantling of strata to form boulders. The bathymetry is shallow and follows the slope of the terrace. The height of the terrace in the highest places does not exceed 3 m. a.s.l. In the immediate submerged area, a large number of fractured boulders have been observed, some of them with marine fauna. Just one boulder has a TF > 1000: its weight is 17.6 t, it is located 2.1 m a.s.l., and a distance from the edge of the cliff of 30.5 m. The rest of the boulders have an average weight of 11 t and, on average, are located 1.4 m a.s.l., and 11.3 m inland from the cliff edge. Some boulders show new impact features and one of them, with incrustated fauna, have been used for C14 age analysis. The orientation of all the boulders is towards NNE, while the dominant swell comes mainly from NE.



Figure 6. (A) Geomorphological scheme of the Sant Antoni area. Roses show the dominant orientation of boulders (left) and the prevailing waves (right). (B,C) Ridges of boulders very close to sea level at Sant Antoni.

3.3. Ibiza: Ses Eres Roges

The outcropping boulders in Ses Eres Roges are located on a low-lying terrace, corresponding to fossil dunes and clay levels that give rise to a sloping coastline characterized by processes of differential dismantling that favor the presence of boulders (Figure 7). We can differentiate clusters of imbricated boulders, isolated boulders, and boulder ridges in the upper areas of the outcrop. The bathymetry in the area is quite gentle and, there is a large number of isolated boulders in the shoreface.

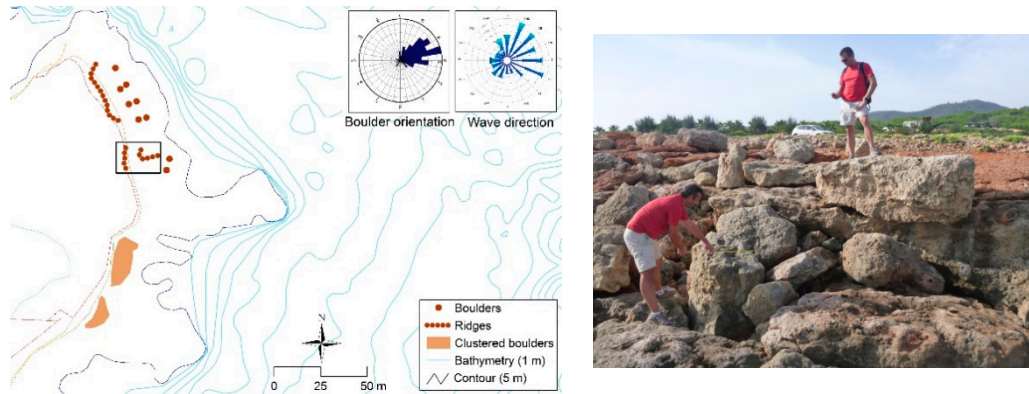


Figure 7. Geomorphological scheme of the Ses Eres Roges area. Roses show the prevailing waves (right) and dominant orientation of boulders (left).

As well as in Sant Antoni, just one boulder has a TF > 1000: its weight is 14.5 t, and it is located 3.5 m a.s.l. and a distance from the edge of the cliff of 25 m. Rest of the boulders have an average weight of 2.3 t, are located 3.1 m a.s.l., and 21.4 m inland from the cliff edge. Some boulders show new impact features and one of them, with incrustated fauna, have been used for C14 age analysis. Average orientation of all the boulders is towards ENE, while the dominant swell comes mainly from the NE.

3.4. Ibiza: Pou des Lleó

The boulders of this site are placed over a littoral platform at an average altitude of 12 m a.s.l. (Figure 8). The slope of the platform reaches 6.4°. The study area shows two units with the presence of boulders and is separated by a small sea entrance. The materials are Middle Triassic limestone, and the presence of boulders is quite conditioned by the degree of fracturing present in the area. Both units show ridges of boulders of metric size. The average weight of boulders is 8.5 t with a maximum of 28 t. Average distance from the cliff edge is 38.6 m with a maximum of 46 m. The dominant swell of this zone comes from NE, while the dominant direction of the imbricated boulders is not well defined.

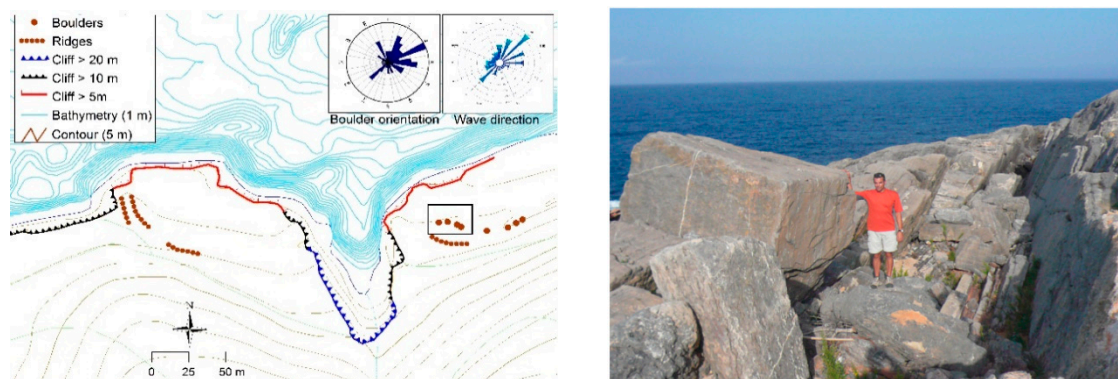


Figure 8. Geomorphological scheme of the Pou des Lleó area. Roses show the dominant orientation of boulders (picture on the right) and the prevailing waves.

3.5. Ibiza: Punta Arabí

The boulders are located over a small peninsula of Cretaceous marly limestones at an average altitude of 14.5 m (Figure 9). The boulders are distributed in several ridges and scattered groups of boulders. The boulders do not present any reworking; neither impact marks are observed. Weight average of the boulders is 4.6 t with a maximum of 7.3 t, and the average distance from the cliff edge is 35 m. The dominant swell for this area is from ENE, while the dominant direction of the imbricated boulders is SE and some of them are imbricated.

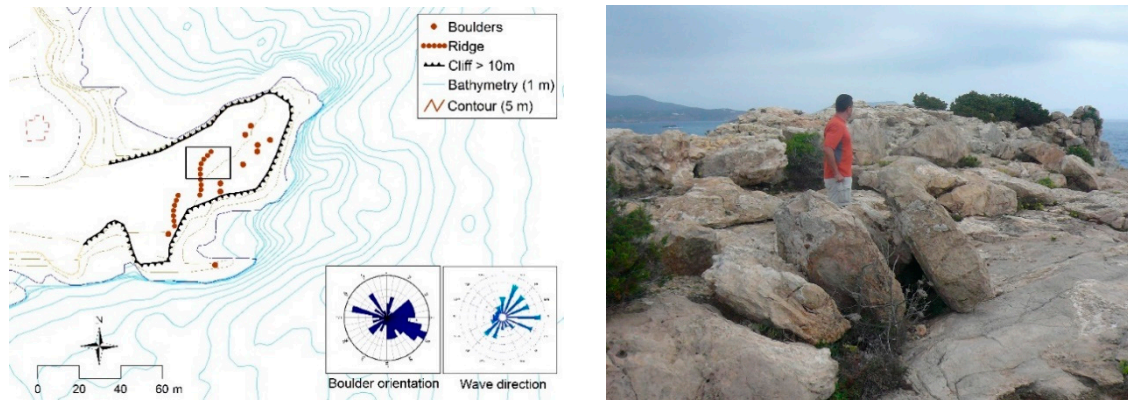


Figure 9. Geomorphological scheme of the Punta Arabí area. Roses show the prevailing waves (left) and dominant orientation of boulders (right).

3.6. Formentera: Punta Prima

The boulders of Punta Prima are located on small peninsula East of Formentera that conforms to a littoral platform from 5 to 15 m a.s.l. (Figure 10). The boulders are situated in the central part of the platform at an average altitude of 11.7 m a.s.l. The average weight of the boulders is 8.7 t, with a maximum of 31.5 t, and their average distance from the edge of the cliff is 83 m. Some groups of imbricated boulders exist, and a ridge in the central part was set. The maximum recorded wave height for this area is 9 m; meanwhile the dominant swell presents an orientation from ENE, the dominant direction of the imbricated boulders is towards the E. The short axes of the boulders correspond to the strata thickness of the denudation areas of the coastal terraces.

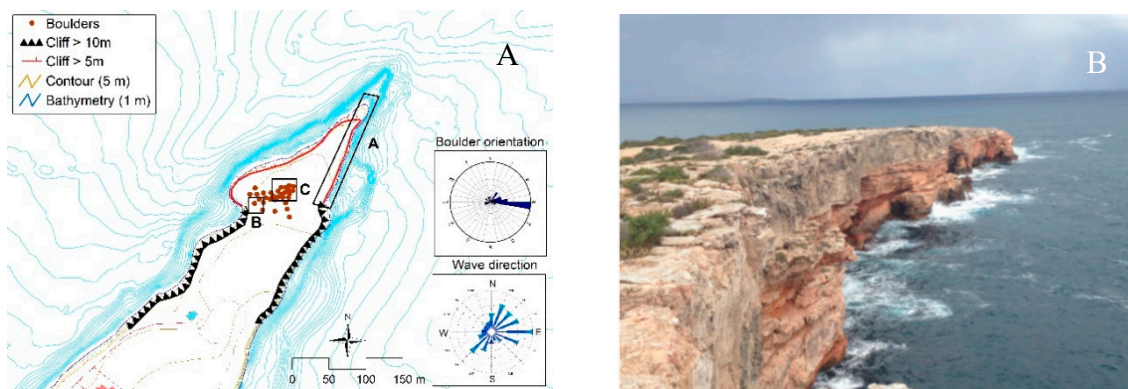


Figure 10. Cont.

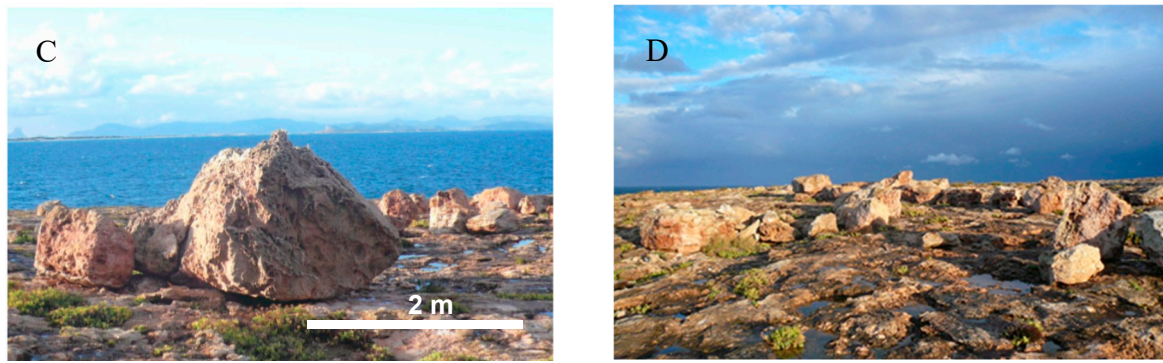


Figure 10. (A) Geomorphological scheme of the Punta Prima area. Roses show the dominant orientation of boulders and the prevailing waves. (B) Cliff on which the analyzed boulders are located. (C) Large block located at 11.5 m a.s.l., and dated in the year 1792 BC. (D) Block ridge located 115 m from the cliff edge, and 12.9 m a.s.l.

3.7. Formentera: Punta de sa Gavina

The geomorphological scheme of Punta de sa Gavina (Figure 11) reflects the presence of different boulders ridges. The boulders have an average weight of 10.7 t; they are at an average distance of 59 m, and an average height of 11.3 m. This area has also large boulders partially covered by an aeolian mantle, and with dominant orientations and imbrications of 254, similar to the boulders analyzed. These partially buried boulders are located 217 m from the cliff ledge and on a tabular platform at 11.5 m a.s.l. No impact marks are observed.

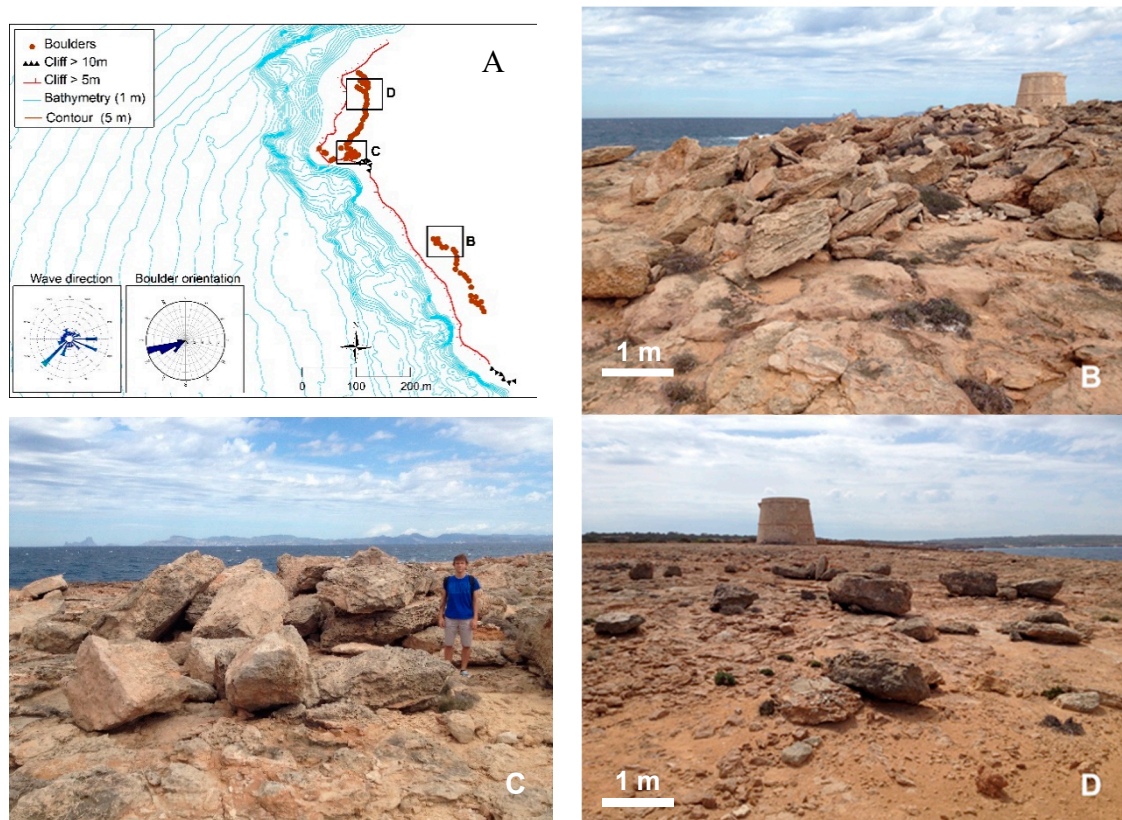


Figure 11. (A) Geomorphological scheme of the Punta de sa Gavina area. Roses show the dominant wave winds (left) and the dominant block orientation (right). (B) Groups of imbricated boulders at 7 m a.s.l., and 25 m from the cliff ledge. (C) Imbricate boulders of large dimensions 37 m from the cornice, and 8.5 m a.s.l. (D) Boulders deposited more than 85 m from the cliff ledge, and 9.5 m a.s.l.

The maximum recorded wave height in this area is 8 m. The dominant swell is from SW, while the dominant direction of the boulders analyzed is WSW.

3.8. Application of Hydrodynamic Equations

The first approach to discriminate storms from tsunamis in the formation of these large boulders is to test the equations which model boulder quarrying by waves. The equations of [9,10] were employed to discriminating between tsunami and storm waves. In Table 4, results of applying Engel and May’s equation are presented for joint-bounded boulders (JBB), and subaerial boulders (SAB) of the seven outcrops studied. H_s (minimum wave height of a swell wave able to move the boulder at sea level) is, in almost all the areas, approximately three times H_t (minimum tsunami water column height needed to move a boulder at sea level). Because H_s is higher to H_{max} (the maximum wave height recorded) and H_{sw} for T50 (significant wave height for a 50-year return period), in all the study sites (excepting Ses Eres Roges and Sant Antoni) storms on Ibiza and Formentera cannot move any boulders with $TF > 1000$, not even the boulders located at sea level. This point agrees with our observations in the field, where the most significant storm waves ever recorded in the Ibiza and Formentera moved none of the boulders we marked in advance (work in progress).

Table 4. Main characteristics of the boulders with $TF > 1000$ from the different study areas. (Alt., average altitude of the boulders, Dist., the average distance from the cliff edge, JBB, joint bounded boulders, R_s —run-up for storm waves, R_t , run-up for the tsunami). In grey, locations dominated by storm-waves action.

Study Area	Alt.	Dist.	Weight	Hc	Hs50	JBB Run-up				Subaerial Run-up		Transport Figure
						Hs	Ht	Rs	Rt	Rs	Rt	
Punta Pedrera	10.0	66.0	8.4	9	11	10.5	3.4	19.5	12.4	11.9	10.4	5319
Sant Antoni	2.1	30.5	17.6	0.5	11	7.8	1.6	8.3	2.1	10.4	3.2	1126
Ses Eres Roges	3.5	25.0	14.5	1	11	6.5	0.9	7.5	1.9	4.9	2.8	172
Pou des Lleó	9.4	38.6	8.5	5.5	11	15	6.5	20.5	12.0	11.6	9.9	3230
Punta Arabí	14.5	35.0	4.6	10	11	11.4	6.2	21.4	16.2	17.6	15.1	2353
Punta Prima	11.7	83.0	8.7	9.5	7	12.2	4.7	21.7	14.2	13.5	12.1	8365
Punta de sa Gavina	11.3	59.0	10.7	9.5	11	12.6	4.5	22.1	14.0	13.1	11.7	7005

On the other hand, tsunami waves with heights less than 6.5 m in Ibiza or less than 4.7 m in Formentera, can move boulders with $TF > 1000$ at sea level. The run-up values given in the text are the sum of H_s (minimum storm water column height) and Alt (the average altitude of boulders), for storm run-ups (R_s) and the sum of H_t (minimum tsunami water column height) and Alt for tsunami run-ups (R_t). In Formentera (Punta Prima, Punta de sa Gavina), for joint bounded boulders, storm run-ups of 22 m are required to explain the position of the boulders, while 14 m tsunami run-ups can explain the same positions. Results in Ibiza requires tsunamis run-ups of 12 m high and or storm run-ups of 20 m. According to these results, a tsunami appears to be a more likely mechanism for transportation and deposition of the boulder field than storm waves.

The run-up of tsunamis on vertical cliffs is several times higher than that occurring on low coastal areas [43]. The run-up is also enhanced due to several factors [44]: (1) by the distance from the tsunami generation area (only 300 km, in our case), (2) the narrowness of the continental shelf (as in Ibiza and Formentera), (3) the fact that the tsunami propagation vector is almost perpendicular to the main shoreline direction, and (4) land morphology, characterized by vertical cliffs with entrances (calas). For these reasons, we think than run-up heights for the Ibiza and Formentera cliffs would have been several times higher than tsunami wave heights. Recent examples in the Balearic Islands confirm the last statement: the tsunami of 2003 had an offshore wave height of 30–40 cm (according to simulations) and reached the western part of Ibiza with a run-up of 3 m, which indicates a multiplying factor of $\times 10$.

3.9. Dating of the Boulders

Just some boulders of Sant Antoni outcrops have incrustated fauna able to be aged by C14 isotope. We sampled a boulder and Conventional age is 310 +/-30 BP, and Calibrated date is 1874–1950 AD with 95.4% probability (High Probability Density Range Method (HPD): MARINE13 from Beta Analytic).

The boulders without incrustated fauna are dated by measuring the karst dissolution features after the block transport. The depth of dissolution pans has been used for an approximate dating of the boulder detachment and transport. Some boulders show the existence of both pre-transport and post-transport dissolution pans. The pre-transport dissolution pans were formed when the boulder formed part of a horizontal bed of the Upper Miocene Reefal Unit. After the transport, the boulder has been tilted, together with the dissolution pan, usually more than 30 degrees due to imbrication. After imbrication, a new dissolution pan develops at an approximate 30 degrees angle concerning the pre-transport dissolution pan. To ensure that it is a real post-transported pan, the existence of an angle of discordance between the stratification of the block, almost horizontal before being ripped, and the surface of the pan, has been verified. Thus, calculating how much time took the post-transport dissolution pan to develop, the age of the boulder transport would be known. According to [45,46] the average value of dissolution rate in the Balearic Islands for dissolution pans is 0.3 mm/yr. Applying this average value of dissolution rate to the mean depth of the dissolution pans (6.8 cm), results in a time-lapse of 227 years, obtaining an age of 1792 AD for Formentera boulders emplacement [47]. This dating shows similar age than the documentary sources of a tsunami registered in 1756 [35] in the municipality of Santanyí (SE Majorca) and with the data analyzed in boulders by C14 on the coast of Minorca [17].

3.10. Discussion

The record of earthquakes offshore from the Algerian coast are extensive (Figure 3). Most of them may generate tsunami waves which reach the southern coasts of the Balearic Islands and, in particular, the Ibiza and Formentera shores. The last event took place in May 2003. Modeled directions by [18] from the N of Africa, corresponding to trajectories S-1 and S-2 (Figure 4), match to the outcrops of boulders analyzed in Ibiza and Formentera Islands.

According to the hydrodynamic equations, two of them, Sant Antoni and Ses Eres Roges, are clearly within reach of swell, while the other five are far out of reach. The existence of tsunamis reaching the coasts of Ibiza and Formentera is unquestionable, because there is recent and also historical evidence. If we prove the existence of boulders transported by tsunamis in the most unfavorable situations for an interpretation of transport by storm waves, it is evident that the boulders deposited in low coast may have a mixed origin: tsunamis and storm waves. Therefore, we must focus the discussion on the characteristics of the boulders identified in Punta Pedrera, Pou des Lleo, Punta Arabí in Ibiza, and Punta Prima and Punta de sa Gavina in Formentera.

The boulders of these outcrops are at average altitudes between 9.4 and 14.5 m a.s.l., at medium distances from the edge of the cliff between 66 and 217 m, and average weights range between 8.4 t and 10.7 t (Table 2). When the equations of Engel and May [10] are applied to these boulders, we get run-ups of around 20 m for the quarry and transport by storm waves of boulders delimited by joints (JBB). For the transport of subaerial boulders, previously uprooted, the run-up values of waves are between 11.6 and 17.6 m. These results are almost impossible to reach with the available data of the wave regime of this area.

Alternatively, the results of the Engel and May [10] formulas (Table 2) for tsunami flows are between 12 and 16.2 m of run-up for boulders delimited by joints (JBB) and between 9.9 and 15.1 m for subaerial boulders. To understand how a tsunami impacts on a cliff, we must know how this flow works. When the tsunami flow hit vertical cliffs, the flow rises progressively until it overtops the cliff and creates fields of boulders plucked from its cornice. The results of the tsunami run-up (R_t) here obtained are adjusted to the models of the water column required for the displacement of each block described by [48]. The deposits analyzed show well-imbricated boulders (Figure 11B)

where the average directions of the boulders coincide with tsunami model directions, adjusting their disposition to the criteria of [42], which argue that this type of imbricated organization is attributable to tsunami events. Thus, the boulders show the result of significant flow events associated with tsunamis, providing evidence of individual and/or multiple events over the same area, with a clear correlation with the tsunami propagation models (Figure 3), and ratified by the application of hydrodynamic equations to establish the water columns (run-up) necessary for the transport and start-up of them (Table 2).

A more integral way of establishing the energy needed to start and transport the boulders is the formula of Scheffers and Kelletal [11], that multiplies the height of the block, the distance to the coastline and its weight (Transport Figure). This equation allows, according to its authors, to better define the difference between the energy of the storm surge and tsunami flows. Ref. [16] determine a threshold of $TF > 250$ for tsunami boulders in Majorca. In our work, for safety, only TF for the biggest boulders ($TF > 1000$) have been used. The boulders analyzed show TF values between 2353 and 8365 in the highest cliffs, while for the lowest, the TF values range between 172 and 1126 (Figure 12 and Table 2).

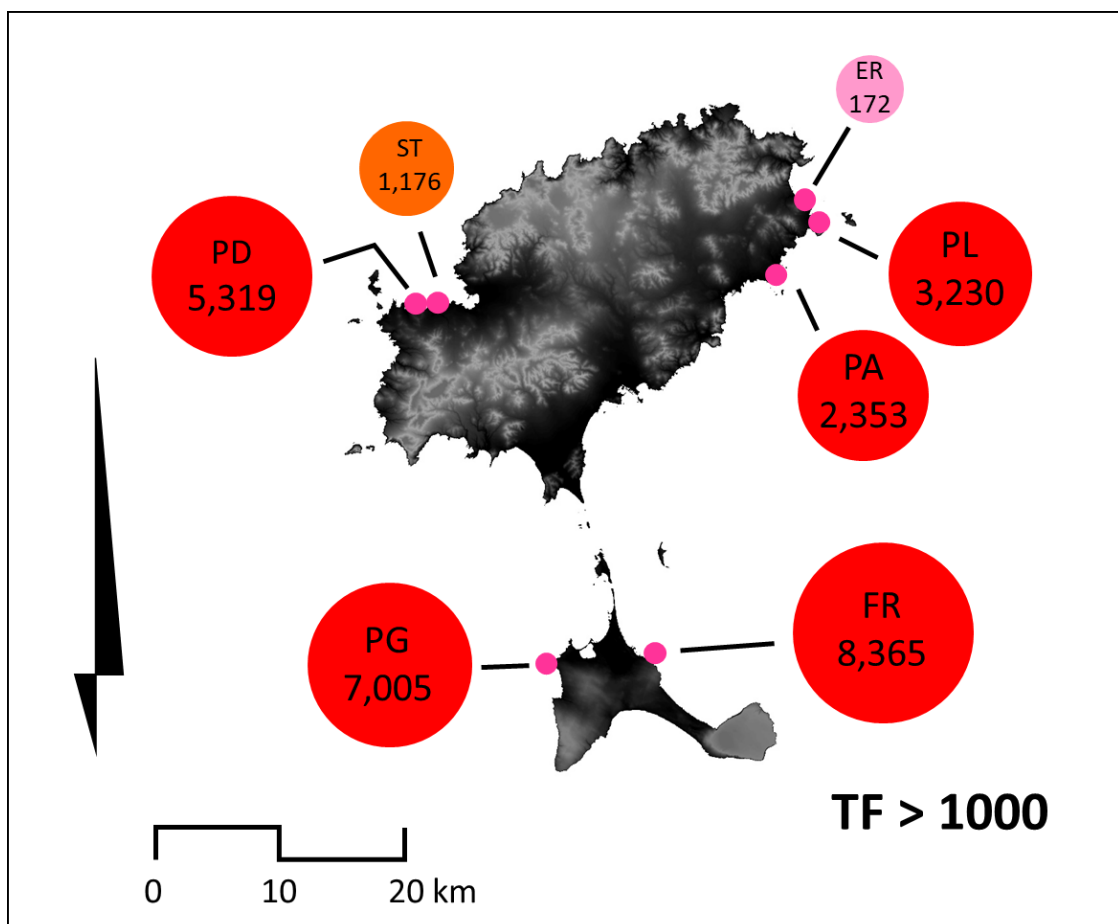


Figure 12. Average values of the Transport Figures for the boulders with $TF > 1000$. (PD, Punta Pedrera, ST, Sant Antoni, ER, ses Eres Roges, PL, Pou desLleò, PA, Punta Arabí, FT, Punta Prima, PG, Punta Gavina).

As shown in Figure 1, most of the outcrops of the boulders in the Balearic Islands, are found on its southern coasts, oriented towards the Algerian coasts. However, both in Minorca and in Ibiza there are some outcrops on its northern coasts, but not in Majorca. In the case of Ibiza, this situation is explained by the diffraction of the tsunami, as happened in the event of 2003 (Figure 3), which produced a maximum elevation in the port of Sant Antoni.

4. Conclusions

The tsunami waves that impact on the Balearic Islands come from the activity of reverse faults on the northern Algeria shelf. There have been tsunami events recently (May 2003), and there is also historical evidence of tsunamis in the past. As a result of the impact of these tsunami waves, both isolated boulders and ridges of boulders of metric size have been deposited at the rocky coasts of Ibiza and Formentera Islands. The radiocarbon dating of the fauna incrustated in some boulders records an event around 1874 (95.4%). Measures of the deepness of post-transport kamenitzas (dissolution basin pools) in Formentera boulders give an age of 1792 AD.

Five littoral boulders outcrops have been analyzed in the island of Ibiza and two more in the island of Formentera. Disposal of the boulders, ten of meters inland from the cliff edge and well away from any source of gravitational origin, restrain their transport from moving inland from the seashore. Lithology and facies are coincident with the ones laying on the upper beds forming the cliffs. In this way, most of the boulders have been quarried and transported inland from the cliff edge. Just very few boulders have incrustated fauna. One of them has been used for radiocarbon dating.

The wave regime of Ibiza and Formentera is characterized by a limited fetch from the northern and southern winds, a 500 km fetch from the SW, and 900 km fetch from the ESE. Wave altitudes reach up to 11 m (Hs50) according to deep water digital buoys data set.

Boulders of five of the outcrops (Punta Pedrera, Pou des Lleó and Punta Arabí in Ibiza and Punta Prima and Punta Gavina in Formentera) are located 12 m a.s.l. on average, at distances between 35 and 217 m from the cliff edge, and have weights between 5 and 10 t (Table 2). Hydrodynamic equations require storm wave heights of 20 m for quarrying the boulders and around 13 m for storm waves to move subaerial boulders already plucked. Transport Figure [11] confirm a tsunami interpretation for the origin of this boulders. Values of TF from two to eight thousand ratify the requirement for a tsunami flow to start and transfer those boulders to their current position and even for their imbrication.

Two outcrops of Ibiza (Sant Antoni and Ses Eres Roges) show boulders between 2 and 3 m a.s.l., 25 to 30 m inland from the sea-shore. Although their weights on average are 17.6 and 14.5 t, respectively, their position could be reached by storm waves. Nevertheless, the tsunami origin of the rest of outcrops obliges to consider a mixed origin for these deposits.

As a conclusion, most of the boulders of the analyzed outcrops are quarried from the cliff edge by tsunami flows. They come from the activity of the faults on the northern Algeria shelf. They hit the Balearic Islands, and, in this case, Ibiza and Formentera coasts.

Supplementary Materials: The following are available online at <http://hdl.handle.net/2445/103318> (last access: June 11, 2019).

Author Contributions: Conceptualization and Methodology, F.X.R.-M., A.R.-P., J.A.M.-P., B.G., and J.M.V.; Fieldwork F.X.R.-M.; Investigation, F.X.R.-M., A.R.-P., J.A.M.-P., B.G., and J.M.V.; Writing—original draft preparation, A.R.P.; Writing—review and editing, B.G.; Visualization, J.A.M.-P.

Funding: This study was supported by the projects CGL2013-48441-P, the CGL2016-79246-P (AEI/FEDER, UE), the CHARMA project (MINECO, ref. CGL2013-40828-R), the PROMONTEC project (MINEICO, ref. 444CGL2017-84720-R) and the CSO20015-64468-P (MINECO/FEDER) project.

Acknowledgments: The authors would like to acknowledge to the staff of the Ses Salines d'Eivissa and Formentera Natural Park: Núria Valverde and Vicent Forteza, for the authorizations to access Punta Gavina.

Conflicts of Interest: The authors declare no conflict of interest.

References

1. Ciavola, P.; Ferreira, O.; Haerens, P.; van Koningsveld, M.; Armaroli, C.; Lequeux, Q. Storm impacts along European coastlines. Part 1: The joint effort of the MICORE and ConHaz Projects. *Environ. Sci. Policy* **2011**, *14*, 912–923. [CrossRef]
2. Scheffers, A.; Scheffers, S. Documentation of Hurricane Ivan on the Coastline of Bonaire. *J. Coast. Res.* **2006**, *22*, 1437–1450. [CrossRef]

3. Goto, K.; Okada, K.; Imamura, F. Characteristics and hydrodynamics of boulders transported by storm waves at Kudaka Island, Japan. *Mar. Geol.* **2009**, *262*, 14–24. [[CrossRef](#)]
4. Biolchi, S.; Furlani, S.; Antonioli, F.; Baldassini, N.; Causon Deguara, J.; Devoto, S.; di Stefano, A.; Evans, J.; Gambin, T.; Gauci, R.; et al. Boulder accumulations related to extreme wave events on the eastern coast of Malta. *Nat. Hazards Earth Syst. Sci.* **2015**, *3*, 5977–6019. [[CrossRef](#)]
5. Morton, R.A.; Richmond, B.M.; Jaffe, B.E.; Gelfenbaum, G. Coarse-clast ridge complexes of the Caribbean: a preliminary basis for distinguishing tsunami and storm-wave origins. *J. Sedim. Res.* **2008**, *78*, 624–637. [[CrossRef](#)]
6. Imamura, F.; Goto, K.; Ohkubo, S. A numerical model for the transport of a boulder by tsunami. *J. Geophys. Res.* **2008**, *113*, C01008. [[CrossRef](#)]
7. Scheffers, A.M.; Kinis, S. Stable imbrication and delicate/unstable settings in coastal boulder deposits: Indicators for tsunami dislocation? *Quat. Int.* **2014**, *332*, 73–84. [[CrossRef](#)]
8. Etienne, S.; Paris, R. Boulder accumulations related to storms on the south coast of the Reykjanes Peninsula (Iceland). *Geomorphology* **2010**, *114*, 55–70. [[CrossRef](#)]
9. Nott, J. Tsunami or storm waves? Determining the origin of a spectacular field of wave emplaced boulders using numerical storm surge and wave models and hydrodynamic transport equations. *J. Coast. Res.* **2003**, *19*, 348–356.
10. Engel, M.; May, S.M. Bonaire's boulder fields revisited: Evidence for Holocene tsunami impact on the Lee-ward Antilles. *Quat. Sci. Rev.* **2012**, *54*, 126–141. [[CrossRef](#)]
11. Scheffers, A.; Kelletat, D. Sedimentologic and geomorphic tsunami imprints worldwide—A review. *Earth-Sci. Rev.* **2003**, *63*, 83–92. [[CrossRef](#)]
12. Furlani, S.; Pappalardo, M.; Gómez-Pujol, L.; Chelli, A. The rock coast of the Mediterranean and Black seas. *Geol. Soc. Lond. Mem.* **2014**, *40*, 89–123. [[CrossRef](#)]
13. Roig-Munar, F.X. Blocs de Tempesta i Tsunami a les Costes Rocoses de les Illes Balears. Anàlisi Geomorfològica i Morfomètrica. Ph.D. Thesis, Departament de Geodinàmica i Geofísica, Universitat de Barcelona, Barcelona, Spain, 2016.
14. Roig-Munar, F.X.; Vilaplana, J.M.; Rodríguez-Perea, A.; Martín-Prieto, J.A.; Gelabert, B. Presencia de bloques de tsunami en los acantilados de Punta Gavina (Formentera, Illes Balears). *Geo-Temas* **2017**, *17*, 223–226.
15. Bartel, P.; Kelletat, D. *Erster Nachweis Holozäner Tsunamis im Westlichen Mittelmeergebiet (Mallorca, Spanien) mit einem Vergleich von Tsunami und Sturmwellenwirkung auf Festgesteinsküsten*; Berichte Forschungs- und Technologiezentrum Westküste der Universität Kiel: Büsum, Germany, 2003; Volume 28, pp. 93–107.
16. Kelletat, D.; Whelan, F.; Bartel, P.; Scheffers, A. New Tsunami evidences in Southern Spain Cabo de Trafalgar and Mallorca Island. In *Geomorfologia Litoral i Quarternari, Homenatge al Professor Vincenç M. Rosselló i Verger*; Sanjaume, E., Matheu, J.F., Eds.; Universitat de València: Valencia, Spain, 2005; pp. 215–222.
17. Roig-Munar, F.X.; Vilaplana, J.M.; Rodríguez-Perea, A.; Martín-Prieto, J.A.; Gelabert, B. Tsunamis boulders on the rocky shores of Minorca (Balearic Islands). *Nat. Hazards Earth Syst. Sci.* **2018**, *18*, 1985–1998. [[CrossRef](#)]
18. Roig-Munar, F.X.; Rodríguez-Perea, A.; Vilaplana, J.M.; Martín-Prieto, J.A.; Gelabert, B. Tsunami boulders in Majorca Island (Balearic Islands, Spain). *Geomorphology* **2019**, *334*, 76–90. [[CrossRef](#)]
19. Álvarez-Gómez, J.A.; Aniel-Quiroga, I.; González, M.; Otero, L. Tsunami hazard at the Western Mediterranean Spanish coast from seismic sources. *Nat. Hazards Earth Syst. Sci.* **2011**, *11*, 227–240. [[CrossRef](#)]
20. Rangheard, Y. The geological history of Eivissa and Formentera. In *Biogeography and Ecology of the Pityusic Islands*; Monographiae Biologicae 52; Kuhbier, H., Alcover, J.A., Guerau d'Arellano Tur, C., Eds.; Springer: Dordrecht, Germany, 1984; pp. 25–104.
21. García de Domingo, A.; Díaz de Neira, J.A.; Gil-Gil, J.; Cabra-Gil, P. *Cartografía y Memoria del Mapa Geológico de España a escala 1:25.000 (Plan MAGNA, 2ª serie) de la Hoja 799 I (Santa Eulària des Riu)*; Servicio de Publicaciones del IGME: Madrid, Spain, 2009.
22. Del Valle, L.; Gómez-Pujol, L.; Fornós, J.J.; Timar-Gabor, A.; Anechitei-Deacu, V.; Pomar, F. Middle to Late Pleistocene dunefields in rocky coast settings at Cala Xuclar (Eivissa, Western Mediterranean): Recognition, architecture and luminescence chronology. *Quat. Int.* **2016**, *407*, 4–13. [[CrossRef](#)]
23. Durand-Delga, M.; Rangheard, Y. Structure de l'île d'Eivissa (Ibiza) et sa place dans le cadre baléare. *Boll. Soc. Hist. Nat. Balears* **2013**, *56*, 25–50.
24. Nozal, F.; Montes, M.; Díaz de Neira, J.A.; Sevillano, A.; Rodríguez-García, A. Cartografía geomorfológica en el Dominio Público Marítimo-Terrestre. *Geo-Temas* **2015**, *15*, 121–124.

25. Roig-Munar, F.X.; Ródriguez-Perea, A.; Martín-Prieto, J.A.; Vilaplana, J.M.; Gelabert, B. El uso de bloques de tormenta y de tsunami como materia prima en las islas Baleares. *Rev. Soc. Geol. España* **2016**, *29*, 79–88.
26. Lionello, P.; Sanna, A. Mediterranean wave climate variability and its links with NAO and Indian Monsoon. *Clim. Dyn.* **2005**, *25*, 611–623. [[CrossRef](#)]
27. Sotillo, M.; Ratsimandresy, A.; Carretero, J.; Bentamy, A.; Valero, F.; González-Rouco, F. A high-resolution 44-year atmospheric hindcast for the Mediterranean Basin: Contribution to the regional improvement of global reanalysis. *Clim. Dyn.* **2005**, *25*, 219–236. [[CrossRef](#)]
28. Bertotti, L.; Cavaleri, L. Analysis of the Voyager storm. *Ocean Eng.* **2008**, *35*, 1–5. [[CrossRef](#)]
29. Puertos del Estado. Available online: <http://www.puertos.es/ca-es/oceanografia/Pagines/portus.aspx> (accessed on 10 May 2019).
30. Cañellas, B. Long-Term Extreme Wave Height Events in the Balearic Sea: Characterization, Variability and Prediction. Ph.D. Thesis, Universitat de les Illes Balears, Mallorca, Spain, 4 May 2010.
31. Papadopoulos, G.A. The development of the National Tsunami Warning System of Greece. *EMSC Newsl.* **2009**, *23*, 20–21.
32. Alasset, J.P.; Hebert, H.; Maouche, S.; Calbini, V.; Meghraoui, M. The tsunami induced by the 2003 Zemmouri earthquake (Mw p 6.9 Algeria): Modelling and results. *Geophys. J. Int.* **2006**, *166*, 213–226. [[CrossRef](#)]
33. Roger, J.; Hébert, H. The 1856 Djielli (Algeria) earthquake and tsunami source parameters and implications for tsunami hazard in the Balearic Islands. *Nat. Hazards Earth Syst. Sci.* **2008**, *8*, 721–731. [[CrossRef](#)]
34. Sahal, A.; Roger, J.; Allgeyer, S. The tsunami triggered by the 21 May 2003 Boumerdès-Zemmouri (Algeria) earthquake: Field investigations on the French Mediterranean coast and tsunami modeling. *Nat. Hazards Earth Syst. Sci.* **2009**, *9*, 1823–1834. [[CrossRef](#)]
35. Fontseré, E. *Notas Sueltas de Sismología Balear*; Publicaciones de la Sección de Ciencias Naturales, Facultad de Ciencias de la Universidad de Barcelona: Barcelona, Spain, 1918; pp. 5–12.
36. Roig-Munar, F.X.; Vilaplana, J.M.; Rodríguez-Perea, A.; Martín-Prieto, J.A.; Gelabert, B. Indicadores geomorfológicos de tsunamis históricos en las costas rocosas de Baleares. *Geo-Temas* **2016**, *16*, 641–644.
37. Martínez-Solares, J.M.; Mezcuca-Rodríguez, J. *Catálogo Sísmico de la Península Ibérica (880 a. C.-1990)*; Dirección General del Instituto Geográfico Nacional: Madrid, Spain, 2002; 253p, Silva and Rodríguez (2014).
38. IDEIB, Infraestructura de Dades Espacials de les Illes Balears. Available online: <https://ideib.caib.es/visor/> (accessed on 5 April 2019).
39. Life Posidonia Project E: 1.5000. Available online: <http://cedai.imedeia.uib-csic.es> (accessed on 22 January 2019).
40. Pignatelli, C.; Sanso, P.; Mastronuzzi, G. Evaluation of tsunami flooding using geomorphologic evidence. *Mar. Geol.* **2009**, *260*, 6–18. [[CrossRef](#)]
41. Nandasena, N.A.K.; Paris, R.; Tanaka, N. Reassessment of hydrodynamic equations: Minimum flow velocity to initiate boulder transport by high energy events (storms, tsunamis). *Mar. Geol.* **2011**, *281*, 70–84. [[CrossRef](#)]
42. Bryant, E. *Tsunami. The Underrated Hazard*, 3rd ed.; Springer: Berlin, Germany, 2014; 222p.
43. Lekkas, E.; Andreadakis, E.; Kostaki, I.; Kapourani, E. Critical Factors for Run-up and Impact of the Tohoku Earthquake Tsunami. *Int. J. Geosci.* **2011**, *2*, 310–317. [[CrossRef](#)]
44. Zhao, X.; Chen, Y.; Huang, Z.; Gao, Y. A numerical study of tsunami wave run-up and impact on coastal cliffs using a CIP-based model. *Nat. Hazards Earth Syst. Sci.* **2017**, 1–17. [[CrossRef](#)]
45. Emery, K.O. Marine solution basins. *J. Geol.* **1946**, *54*, 209–228. [[CrossRef](#)]
46. Gómez-Pujol, L. Patrons, Taxes i Formes d’Erosió a les Costes Rocoses Carbonatades de Mallorca. Ph.D. Thesis, Departament de Ciències de la Terra, Universitat de les Illes Balears, Mallorca, Spain, April 2006.
47. Roig-Munar, F.X.; Martín-Prieto, J.A.; Vilaplana, J.M.; Rodríguez-Perea, A.; Gelabert, B. Presencia de bloques de tsunamis en acantilados de Punta Prima (Formentera). In *Comprendiendo el Relieve: Del Pasado al Futuro*; Durán, J.J., Montes Santiago, M., Robador, A., Salazar, Á., Eds.; Instituto Geológico y Minero de España: Madrid, Spain, 2016; pp. 571–578.
48. Switzer, A.D.; Burston, J.M. Competing mechanisms for boulder deposition on the southeast Australian coast. *Geomorphology* **2010**, *114*, 42–54. [[CrossRef](#)]

